RNA Sequencing Reveals Transcriptomic Changes in Tobacco (*Nicotiana Tabacum*) Following *NtCPS2* Knockout

Shixiao Xu
Henan Agricultural University
Lingxiao He
Henan Agricultural University
Huabing Liu
China Tobacco Zhejiang Industry
Changhe Cheng
China Tobacco Zhejiang Industry
Dongfang Cai
Henan Academy of Agricultural Sciences
Jutao Sun
Henan Agricultural University
Tiezhao Yang
Henan Agricultural University
Gang Xue (xuegangtobacco@163.com)
Henan Agricultural University
Qingquan Xu
China Tobacco Zhejiang Industry

Research article

Keywords: CRISPR-Cas9, Nicotiana tabacum, RNASeq, Labdanoid diterpenes, cis-Abienol, Genome editing, terpenoids.

Posted Date: October 7th, 2020

DOI: https://doi.org/10.21203/rs.3.rs-76752/v1

Abstract

Background: Amber-like compounds form in tobacco (*Nicotiana tabacum*) during leaf curing and impact aromatic quality. In particular, *cis*-abienol, a polycyclic labdane-related diterpenoid, is of research interest as a precursor of these compounds. Glandular trichome cells specifically express copalyl diphosphate synthase (*NtCPS2*) at high levels in tobacco, which, together with *NtABS*, are major regulators of *cis*-abienol biosynthesis in tobacco.

Results: To identify the genes involved in the biosynthesis of *cis*-abienol in tobacco, we constructed transgenic tobacco lines based on an *NtCPS2* gene-knockout model, using CRISPR/Cas9 genome-editing technology to inhibit *NtCPS2* function *in vitro*. In mutant plants, *cis*-abienol and labdene-diol contents decreased, whereas gibberellin and abscisic acid (ABA) contents increased compared with those in wild-type tobacco plants. RNA sequencing analysis revealed the presence of 9,514 differentially expressed genes (DEGs; 4,279 upregulated, 5,235 downregulated) when the leaves of wild-type and *NtCPS2*-knockout tobacco plants were screened. Among these DEGs, the genes encoding *cis*-abienol synthase, ent-kaurene oxidase, auxin/ABA-related proteins, and transcription factors were found to be involved in various biological and physiochemical processes, including diterpenoid biosynthesis, plant hormone signal transduction, plant-pathogen interactions, etc.

Conclusions: Our findings provide clues to the molecular regulatory mechanism underlying *NtCPS2* activity, allowing for a better understanding of the interactions among related genes in tobacco.

Background

Aroma is an important attribute of tobacco (*Nicotiana tabacum* L.) leaves. It is an indicator of tobacco quality and influenced by a variety of chemical components [1]. An important aromatic substance in tobacco-leaf surface secretions is *cis*-abienol, which belongs to the labdanoid diterpenoid family [2, 3]. Previous studies have reported that *cis*-abienol plays an important role in determining the aromatic characteristics of tobacco, and it is an important precursor in the chemical synthesis of amber-like substances [4–6], which can affect aromatic quality. Furthermore, *cis*-abienol is involved in plant resistance to insects [7, 8] and diseases [9]. Therefore, it is important to explore the *cis*-abienol synthesis pathway and regulatory genes in tobacco, to better understand how to create disease-resistant tobacco varieties with high-quality or characteristic aromas upon flue-curing.

The biosynthesis of *cis*-abienol in tobacco was initially reported to be controlled by a single gene, *Abl* [10, 11], which is located on chromosome A [12]. Subsequently, Vontimitta *et al*. [13] used 117 doubled haploid lines and simple sequence repeat molecular markers to locate the genes regulating *cis*-abienol and sucrose ester accumulation, and found that both genes are located on chromosome A. The genetic distance between two genes is 8.5 cM, and a total of 17 pairs of markers can be found in the linkage group. Among them, PT10324 and *Abl* are totally separated. The markers beside *Abl* are PT55091 and PT61373, with distances of 2.02 and 0.6 cM, respectively [13]. Copalyl diphosphate synthase 2 (CPS2)

from the angiosperm *Cistus creticus* subsp. *creticus* was first analyzed through prokaryotic expression and dephosphorylation. Then, gas chromatography-mass spectrometry (GC-MS) analysis revealed that CPS2 catalyses the formation of 13(E)-labden-8-ol-15-diphosphate, implying that *CPS2* is involved in the biosynthesis of *cis*-abienol [14]. In gymnosperms, *cis-abienol synthase* (*ABS/KS*) contains both class I and class II functional domains, as shown by cloning and characterizing the gene from balsam fir (*Abies balsamea*) via transcriptome sequencing [15]. Sallaud *et al*. [16] cloned *NtCPS2* and *NtABS* from tobacco and showed that both genes are involved in the biosynthesis of *cis*-abienol, which involves two steps. First, CPS-like catalytic activity yields 8-hydroxy-copalyl diphosphate with a normal configuration, which can then be converted to *cis*-abienol by the *NtABS* product [16–18]. No other diterpenoid synthase has been reported to be able to use 8-hydroxy-copalyl diphosphate as a substrate in dicotyledons to date. In addition, promoter analysis of *NtCPS2* showed that it could drive the expression of the *GUS* gene in glandular hairs [16, 19, 20]. The identification of *NtCPS2* and *NtABS* is of great significance for breeding high-quality tobacco and future microbial metabolic engineering. From this knowledge base, other diterpenoid-synthesising genes can be cloned and identified.

Among tobacco types, *cis*-abienol accumulates at different levels. It is mainly found in oriental and cigar tobacco but not in flue-cured tobacco, Burley tobacco, or Maryland tobacco [1, 16, 21]. To study the variation in *cis*-abienol content among different types of cultivated tobacco, 157 varieties of tobacco with or without *cis*-abienol were selected, and the expression levels of *NtCPS2* and *NtABS* were analyzed [16]. *NtABS* cDNA sequences did not differ among tobacco varieties, but two distinct polymorphisms were found in *NtCPS2* cDNA: an 8-bp insertion at position 275 and a G-T transversion at position 292 of *NtCPS2.* Both of these result in a stop codon, which leads to early termination and shortening of the encoded peptide chain. Because the encoded protein loses its active site, it also loses its original function [16]. Thus, *NtCPS2* is key for *cis*-abienol biosynthesis. However, the mechanism by which the metabolic pathway of labdanoid diterpenoids regulate *NtCPS2* in tobacco and the effects of *NtCPS2* knockout on other metabolic pathways are still unknown.

In this study, we used CRISPR/Cas9 gene-editing technology to knock out *NtCPS2*. The CRISPR/Cas9 *NtCPS2* expression vector was constructed from the high-aroma strain 8306, and transformed *NtCPS2*-knockout plants were obtained. A high-throughput RNA sequencing (RNA-seq) technique was used to compare expression profiles between mutant and 8306 plants. Sequencing results were verified using fluorescence quantitative polymerase chain reaction (PCR), and physiological changes and transcriptional inheritance were analyzed. By elucidating the function of the *NtCPS2* gene and the molecular mechanisms underlying the regulation of its related genes, high-aroma tobacco varieties can be cultivated.

Results

Targeted Mutagenesis of NtCPS2 by CRISPR/Cas9 in Tobacco

In this study, Cas9 gene was optimised to edit the tobacco genome. To generate Cas9-induced mutations in *NtCPS2*, a vector was designed that harboured chimeric guide RNA (gRNA) to guide Cas9 to target sequences where it bound and cleaved genomic DNA to generate double-strand breaks [22]. Two target sites of *CPS2* were selected (Supplementary Fig. 1). The gRNA for each target site, which was generated by overlap-extension PCR. Cas9 were subcloned into a single expression vector [23]. The Cas9 and gRNA expression cassette was located in one expression vector (pRGEB32-Cas9-NPT II-*CPS2*-gRNA). Through the *Agrobacterium tumefaciens*-mediated method, 36 transformed regenerated plants in the T_0 generation were obtained. After amplification with target-specific primers, all positive samples were sequenced to assess the mutation efficiency. Of 36 plants, eight were transgenic lines. Most of the transgenic lines had a single-base insertion of A, C, or T at Target 2. Thus, as the peptide chain was being formed, the stop codon was encountered early in the process, and the translated amino-acid chain was greatly shortened. To test the heritability of the mutations, homozygous transgenic plants in the T_0, T_1, and T_2 generations were analyzed. Detailed information about the homozygous T_2 plants (M1–M9) is shown in Fig. 1A, and these plants were used for the following experiments.

NtCPS2 Knockout Affects cis-Abienol Content

To verify whether the gene mutations caused changes in gene expression, quantitative real-time PCR (qRT-PCR) was used to detect expression levels of *NtCPS2* in the leaves of mutant and wild-type (8306) plants. The results showed that *NtCPS2* expression decreased significantly in transgenic plants compared to wild-type plants (Fig. 1B). To detect changes in *cis*-abienol content in the leaves, exudates were collected from the mutant plants and analyzed using GC-MS. Contents of *cis*-abienol also decreased significantly in mutant plants compared to wild-type plants (Fig. 1C). The results indicate that *NtCPS2* is one of the key genes regulating the *cis*-abienol biosynthesis pathway, and *NtCPS2* knockout results in low levels of *cis*-abienol biosynthesis and accumulation. *NtABS* is another key gene involved in *cis*-abienol biosynthesis [16]. A previous study reported that *cis*-abienol was detected in plants expressing both *NtCPS2* and *NtABS* but not in plants expressing just one of the two genes [16]. *NtABS* expression was weak in the mutant plants compared to the wild-type plants, implying that *NtCPS2* knockout negatively influenced *NtABS* expression. This is possibly because *NtCPS2* is located upstream of *NtABS* in the *cis*-abienol biosynthesis pathway.

NtCPS2 Has a Minor Effect on the Development of Glandular Trichomes in Tobacco

Agronomic characteristics were analyzed to assess the mutant phenotypes (Fig. 2 and Supplementary Fig. 2). Differences in plant height, internode length, number of leaves, and stem girth between mutant and wild-type plants did not exhibit the same trend. T2-2 mutants had longer internodes and wider stems than other mutants and wild-type plants, whereas all mutants except for T2-1 had shorter plant heights than the wild-type plants (Supplementary Fig. 2). These results indicate that *NtCPS2* expression does not strongly affect tobacco plant morphology. As *NtCPS2* is specifically expressed in glandular cells [16], the morphology of the glandular trichomes on the largest leaf of each plant was examined. Both the length

and width of the largest leaf were significantly shorter in mutant plants compared to wild-type plants. The average diameter of glandular trichomes was smaller in mutant plants, especially T2-1, whereas both longer and shorter glandular trichomes were observed in mutant plants compared to wild-type plants (Fig. 2). Other trichome characteristics, such as numbers of long and short trichomes, did not differ significantly between mutant and wild-type plants (data not shown). Thus, in the absence of *NtCPS2* expression in tobacco plants, the diameter of glandular cells and the area of the largest leaf decrease, but not the length of glandular trichomes. The T2-1 line was selected and used to profile transcriptomic changes after *NtCPS2* knockout in tobacco 8306.

Overview of Transcriptome Sequencing

To profile gene expression after *NtCPS2* knockout, RNA-seq libraries were constructed for the mutant and wild-type plants. Six samples of each line were sequenced, and 41.64 G of clean data was obtained. In total, 6.70–7.02 G of effective data was collected from each sample, with a Q30 distribution of 94.29–94.91%, and an average GC content of 43.41%. More than 95.58% of the clean reads had quality scores that met the Q30 criterium (probability of base-calling error = 0.1%) [24]. Furthermore, the GC content ranged from 43.15–43.66%. The sequencing data are summarised in Table 1.

Table 1
Summary of RNA-sequencing outcomes.

Sample	Raw reads	Clean reads	Raw bases	Clean bases	Q30 (%)	GC (%)
Con1	49.05 M	47.90 M	7.36 G	6.89 G	94.60	43.46
Con2	49.76 M	48.74 M	7.46 G	7.02 G	94.88	43.25
Con3	47.66 M	46.51 M	7.15 G	6.70 G	94.29	43.30
L1	49.71 M	48.57 M	7.46 G	6.97 G	94.67	43.66
L2	49.77 M	48.72 M	7.47 G	6.99 G	94.88	43.41
L3	49.70 M	48.62 M	7.45 G	6.97 G	94.85	43.47
Not: Con, wild type; L, mutant.						

Analysis of Differentially Expressed Genes (DEGs) and Their Functions

Volcano plots were used to assess the variation in gene expression between mutant and wild-type plants (Fig. 3A). In total, 9,514 DEGs were detected. Among them, 4,279 were upregulated and 5,235 were downregulated in the transgenic tobacco plant compared to 8103 using the thresholds $p < 0.05$ and $|\log_2(\text{fold change [FC]})| > 1$ (Fig. 3B).

Kyoto Encyclopedia of Genes and Genomes (KEGG) and Gene Ontology (GO) pathway analyses of the differentially expressed mRNAs were performed to determine the functions of the DEGs. The 20 most

significantly enriched pathways (lowest *q* values) according to KEGG metabolic pathway annotation were examined in detail (Fig. 4A). Based on GO analysis, the DEGs were most likely to be associated with biological processes (Fig. 4B) and cellular components (Fig. 4C). A large percentage of the DEGs was assigned to the categories metabolic process, cellular process, catalytic activity, binding, and single-organism process, with only a few genes assigned to channel regulator activity, cell killing, and protein tag. The DEGs involved in the pathways for diterpenoid biosynthesis, plant hormone signal transduction, and plant-pathogen interactions were analyzed in detail.

Validation of Selected DEGs Using qRT-PCR

To validate the RNA-seq data, 12 DEGs, including genes involved in *cis*-abienol and gibberellin (GA) biosynthesis as well as genes related to plant-pathogen interactions and other hormone signalling pathways, were selected randomly for qRT-PCR analysis. The gene-expression patterns as determined using qRT-PCR were consistent with those determined via transcriptome sequencing (Fig. 5). FC values differed between qRT-PCR and RNA-seq, possibly due to differences in the sensitivity of each method or because different samples were used for qRT-PCR and RNA-seq.

Expression Levels of Genes Related to cis-Abienol Biosynthesis Decreased Significantly in Mutant Plants

NtCPS2 (Nitab4.5_0001630g0010) was identified as a DEG via RNA-seq, and its expression level was 9.27-fold lower in the mutant compared to the wild type. The expression level of another key gene related to *cis*-abienol biosynthesis, *NtABS* (Nitab4.5_0015240g0010), also decreased 2.43-fold in the mutant. *NtCPS2* and *NtABS* operate in succession to synthesise *cis*-abienol [16]. When both *NtCPS2* and *NtABS* are expressed, *cis*-abienol is synthesised and can be detected in plants. However, *cis*-abienol synthesis does not occur in plants that express only one of these genes [16]. *NtCPS2* encodes 8-hydroxy-copalyl diphosphate synthase, which synthesises 8-hydroxy-copalyl diphosphate, and *NtABS* encodes a kaurene synthase-like (KSL) protein, abienol synthase, which uses 8-hydroxy-copalyl diphosphate to produce *cis*-abienol. Our results indicate that weak expression of *NtCPS2* directly or indirectly results in a decrease in the expression level of *NtABS* and consequently, low *cis*-abienol contents. Another putative *cis*-abienol synthase (Nitab4.5_0008024g0010) was also found to be downregulated in the mutant, indicating that this enzyme may have the same substrate as *NtABS* and thus be involved in the *cis*-abienol biosynthesis pathway. By contrast, other putative *cis*-abienol synthases, including Nitab4.5_0004164g0070 and Nitab4.5_0004164g0010, were found to be upregulated in the mutant. These two enzymes may have other functions in tobacco. Other DEGs involved in the *cis*-abienol biosynthesis pathway were also identified (based on KEGG analysis) and had lower expression levels in the mutant (Fig. 4). This included *KSL4* (Nitab4.5_0000029g0200, FC = 2.43) and genes predicted to encode ent-kaur-16-ene synthase (Nitab4.5_0002280g0060, FC = 5.61; and Nitab4.5_0002862g0030, FC = 1.57). As with *KSL4*, *NtABS* is a KSL gene (Table 2). Hence, *KSL4* and genes that putatively encode ent-kaur-16-ene synthase may be involved in *cis*-abienol biosynthesis. This needs to be verified in future work.

Table 2
Genes related to diterpenoid biosynthesis that are differentially expressed between *NtCPS2*-knockout and 8306 plants.

Gene name	Gene ID	log_2FC	Protein properties
CPS2	Nitab4.5_0001630g0010	-3.21	PREDICTED: copal-8-ol diphosphate hydratase, chloroplastic
KSL4	Nitab4.5_0000029g0200	-1.21	PREDICTED: ent-kaur-16-ene synthase, chloroplastic isoform X3
DLO2	Nitab4.5_0000129g0310	-2.53	PREDICTED: gibberellin 2-beta-dioxygenase 8-like
GA2OX2	Nitab4.5_0000222g0140	-5.09	PREDICTED: gibberellin 2-beta-dioxygenase 2
GA2OX1	Nitab4.5_0000923g0050	-3.82	PREDICTED: gibberellin 2-beta-dioxygenase 1-like
GA2OX2	Nitab4.5_0001013g0080	-2.88	PREDICTED: gibberellin 2-beta-dioxygenase 2-like
KAO2	Nitab4.5_0001476g0100	4.06	PREDICTED: ent-kaurenoic acid oxidase 1-like isoform X2
GA20OX2	Nitab4.5_0001573g0060	2.08	gibberellin 20 oxidase 1-like
GA2OX1	Nitab4.5_0002209g0240	-1.46	gibberellin 2-beta-dioxygenase 1-like
KO	Nitab4.5_0002280g0060	-2.49	PREDICTED: ent-kaurene oxidase, chloroplastic
GA2	Nitab4.5_0002862g0030	-1.19	PREDICTED: ent-kaur-16-ene synthase, chloroplastic-like isoform X1
KS1	Nitab4.5_0004164g0010	1.46	PREDICTED: *cis*-abienol synthase, chloroplastic-like
TPS1	Nitab4.5_0004164g0070	3.00	PREDICTED: *cis*-abienol synthase, chloroplastic-like
GA2	Nitab4.5_0008024g0010	-1.20	PREDICTED: *cis*-abienol synthase, chloroplastic-like
CPS1	Nitab4.5_0010312g0010	3.60	PREDICTED: ent-copalyl diphosphate synthase, chloroplastic-like isoform X1
ABS	Nitab4.5_0015240g0010	-1.28	*cis*-abienol synthase, chloroplastic

Note: FC, fold change.

GA Biosynthesis Increased Significantly in Mutant Plants

According to diterpenoid biosynthesis pathways, the same substrate, geranylgeranyl pyrophosphate (GGPP), is used for *cis*-abienol and GA synthesis. In this study, most of the DEGs involved in GA biosynthesis were strongly upregulated in the mutant, including *KAO2* (Nitab4.5_0001476g0100, FC = 16.67), *KS1* (Nitab4.5_0004164g0010, FC = 2.76), and *CPS1* (Nitab4.5_0010312g0010, FC = 12.14) (Table 2). From these genes, ent-copalyl diphosphate synthase 1 (encoded by *CPS1*) and ent-kaurene

synthase (encoded by *KS1*) were found to separately catalyse the synthesis of ent-kaurene from GGPP. However, *KO* (encodes ent-kaurene oxidase, which converts ent-kaurene to kaur-16-en-18-oate) expression was downregulated in the mutant. DEGs participating in the latter stages of the pathway, such as *KAO2* and $GA20_{OX2}$, were upregulated compared to the wild type. KO and KAO belong to the CYP701A, P450, and CYP88A clade. Accordingly, KAO is localised in the endoplasmic reticulum, whereas KO is localised in both the endoplasmic reticulum and plastid envelope [25]. The differential expression of *KO1* and *KAO2* in response to *NtCPS2* knockdown was explored further. GA contents in mutant plants were also analyzed via GC-MS. The results showed that the GA contents in transgenic plants were significantly lower than those in wild-type plants (Fig. 6). GA12 is considered the precursor of all GAs in plants [26], and other GA forms are produced through oxidative steps catalysed by GA12. Genes involved in the production of these GA forms were up- and downregulated in the mutant.

Changes in Abscisic Acid (ABA) Biosynthesis and Signal Transduction in Mutant Plants

In carotenoid biosynthesis pathways, GGPP is also a substrate for ABA synthesis. RNA-seq analysis showed that four *PSY* genes (encoding phytoene synthases) were upregulated at the first step, which involves GGPP, in the mutant compared to the wild type. PSY is a transferase enzyme that is involved in the biosynthesis of carotenoids. It catalyses the conversion of GGPP to phytoene. Two genes encoding LCYs (lycopene epsilon cyclases) were also upregulated in the mutant at the next step. These results indicate that *NtCPS2* knockout positively regulates ABA synthesis, likely because substrate competition decreases. In addition, two ABA 8'-hydroxylases, which are involved in ABA degradation, were downregulated in the mutant. In the ABA signal transduction pathway, five of six ABA receptors (PYLs), which inhibit the expression of protein phosphatase 2C, were upregulated in the mutant. At the next step, serine/threonine-protein kinase expression was upregulated in the mutant. This might have been related to stress responses and stomatal opening and closure in tobacco leaves.

Transcriptomic Analysis of Genes Involved in Plant-pathogen Interactions

In plants, *cis*-abienol may participate in insect resistance and disease resistance [27]. Plant resistance to pathogen attack can induce the accumulation of pathogenesis-related proteins (PRs) that contribute to systematically acquired resistance. In this study, *PRs* were identified through RNA-sEq. Of 17 *PRs*, 14 (82.35%) were significantly upregulated in the mutant than in the wild type, including genes that encode PR proteins 1A, B, and C (Table 3). Among the 17 families of PRs, PR 1–5, 9–11 and 17, were related to the acquisition of defence against the pathogen infections. In addition, calcium is involved in regulating diverse physiological processes as a second messenger [28]. Results of transcriptomic analysis revealed that, 15 of 19 CDPKs and most CAM/CML were significantly downregulated upon *NtCPS2* knockout and low content of *cis*-abienol, which disturbed the balance among active oxygen species, including rubidium hydroxide, reactive oxygen species, and nitric oxide synthase.

Table 3
Properties of DEGs encoding pathogenesis-related proteins.

Gene name	Gene ID	log_2FC	Protein properties
PRB1	Nitab4.5_0003771g0010	4.52	Pathogenesis-related protein 1A
OSM34	Nitab4.5_0004097g0050	3.76	PREDICTED: pathogenesis-related protein R minor form
PRB1	Nitab4.5_0014031g0010	3.51	PREDICTED: pathogenesis-related protein 1B-like
-	Nitab4.5_0006088g0020	3.46	PREDICTED: pathogenesis-related protein PR-4B
-	Nitab4.5_0018960g0010	3.35	PREDICTED: pathogenesis-related protein PR-4B
-	Nitab4.5_0008835g0020	3.27	PREDICTED: pathogenesis-related protein STH-2-like
-	Nitab4.5_0004861g0030	3.24	PREDICTED: pathogenesis-related protein 1C-like
PRB1	Nitab4.5_0004861g0040	3.16	PREDICTED: pathogenesis-related protein 1C
-	Nitab4.5_0008375g0050	3.06	PREDICTED: pathogenesis-related protein STH-2-like
HEL	Nitab4.5_0009495g0020	2.73	PREDICTED: pathogenesis-related protein PR-4A
TL1	Nitab4.5_0008011g0010	2.29	PREDICTED: pathogenesis-related protein 5-like isoform X1
-	Nitab4.5_0000194g0120	2.17	PREDICTED: pathogenesis-related protein STH-2-like
CRF2	Nitab4.5_0000105g0290	2.06	PREDICTED: pathogenesis-related genes transcriptional activator PTI6-like
CRF2	Nitab4.5_0002902g0060	1.11	PREDICTED: pathogenesis-related genes transcriptional activator PTI6-like
MOS11	Nitab4.5_0002073g0060	-1.47	PREDICTED: pathogenesis-related protein PRMS-like
CRF2	Nitab4.5_0000586g0010	-2.67	PREDICTED: pathogenesis-related genes transcriptional activator PTI6-like
CRF2	Nitab4.5_0007730g0010	-2.72	PREDICTED: pathogenesis-related genes transcriptional activator PTI6-like

Discussion

Aromatic characteristics of tobacco are improved by *cis*-abienol, which belongs to the labdane diterpenoid family. Although the genes encoding the enzymes participating in the two steps of *cis*-abienol biosynthesis have been cloned in tobacco [16], the function and regulatory mechanism of *NtCPS2* are

less well-understood. By knocking out *NtCPS2*, whose product catalyses the first reaction in the *cis*-abienol biosynthesis pathway, we were able to examine how *cis*-abienol biosynthesis and other related metabolic pathways are controlled. The regulatory network is shown in Fig. 7.

NtCPS2 Plays a Limited Role in the Biosynthesis of cis-Abienol and Other Terpenoids

Mutations in *NtCPS2* were previously reported to be strongly correlated with the absence of *cis*-abienol and labdene-diol in tobacco or a decrease in their levels [16]. In *N. sylvestris*, *cis*-abienol is accumulated when both *NtCPS2* and *NtABS* are expressed [16]. In this study, we generated *NtCPS2*-knockout tobacco lines using the CRISPR-Cas9 method. In mutant plants that weakly express *NtCPS2*, the levels of *cis*-abienol produced decreased (Fig. 1). *NtABS* is involved in the second step of *cis*-abienol biosynthesis, and its expression levels also decreased (Fig. 5A). The decreased expression of both these genes might have resulted in low levels of the intermediate 8-hydroxy-copalyl diphosphate being accumulated and the cessation of *cis*-abienol production downstream (Fig. 1C). The results indicate that *NtCPS2* plays a key role in *cis*-abienol biosynthesis; thus, downregulated gene expression leads to an inactivation of the *cis*-abienol biosynthesis pathway.

The precursor GGPP, which participates in the first step of the pathway, is a common precursor for the biosynthesis of not only diterpenoids (including *cis*-abienol and labdene-diol) but also GA, carotenoids (including ABA), and the phytolchain of chlorophyll [29]. When NtCPS2 is absent, GGPP is not catalysed to produce 8-hydroxy-copalyl diphosphate, and other reactions that use GGPP as a substrate are enhanced. During GA biosynthesis in *Arabidopsis*, GGDP is converted to ent-kaurene in a two-step reaction catalysed by CPS and KS, which are encoded by *AtCPS* and *AtKS*, respectively [30, 31]. In this study, *NtCPS1* and *NtKS1* expression levels were upregulated after *NtCPS2* knockout, and GA production, which occurs downstream, increased in the leaves of mutant plants (Fig. 6). In terms of carotenoid biosynthesis, genes (including *phytoene synthase 2* and *lycopene epsilon cyclase*) involved in converting GGPP to phytoene were upregulated after *NtCPS2* knockout. Overall, reactions that consume GGPP as a substrate were enhanced. The results indicate that *NtCPS2* knockout also contributes to the biosynthesis of other terpenoids depending on the same substrate. Future studies can verify this hypothesis by overexpressing *NtCPS2* and/or *NtABS.*

Plants with Mutations in NtCPS2 Still Exhibit Wild-type Morphology

Diterpenoids such as cembranoid diterpenes and labdanoid diterpenes from tobacco-leaf exudates significantly influence cigarette-smoke characteristics and flavour profiles [2, 3]. To our knowledge, no previous studies on the effects of *cis*-abienol on the growth and development of tobacco plants have been reported. We found that the mutant and wild-type morphology did not differ much, except for the diameter of glandular trichomes. This indicates that *NtCPS2* knockout and the subsequent decrease in *cis*-abienol do not affect tobacco plant morphology. However, the contents of other chemical substances

(including GA and ABA) may change in mutants. Mutants had lower levels of GA and did not exhibit the GA-overdose morphology. In *Arabidopsis*, CPS- and/or KS-overexpressing mutants also did not exhibit the GA-overdose morphology [32]. This suggests that levels of bioactive GA in these plants likely did not change. Transcriptomic analysis showed that the expression of $GA20_{OX2}$ was upregulated, whereas that of $GA2_{OX4}$, $GA2_{OX2}$, and $GA2_{OX1}$ was downregulated (Table 2). Wild-type *Arabidopsis* plants treated with exogenous GA and transgenic plants overexpressing the downstream GA-biosynthesis gene $AtGA20_{ox1}$ both exhibited aspects of GA-overdose morphology [33]. The differential regulation of $GA20_{OX}$, $GA2_{OX4}$, $GA2_{OX2}$, and $GA2_{OX1}$ might resulted in different types of GA being accumulated at different levels; thus, overall levels of bioactive GA may not change much, and plants may not exhibit a GA-underdose morphology.

cis-Abienol May Participate in Tobacco Disease Resistance

Labdanoid diterpenes may exhibit defence-related activities such as antifungal [34] and insecticidal [7, 8] activities [27, 35]. The application of *cis*-abienol to the roots of tobacco, tomato, and *Arabidopsis* at a concentration of 100 μmol/L can induce the expression of resistance genes and inhibit bacterial wilt disease [27]. *In vitro* experiments showed that concentrations of *cis*-abienol and related diterpenoids in the range 0.01–100 mg/kg can inhibit the growth of *Phytophthora nicotianae* in tobacco. However, upon examination of the *cis*-abienol biosynthesis pathway, we conclude that the accumulation of *cis*-abienol is not related to disease resistance in tobacco plants. Under field conditions, *cis*-abienol does not have an effect on diseased leaves in tobacco. Therefore, it is unclear whether genes related to *cis*-abienol synthesis contribute to resistance against *P. nicotianae* in tobacco. A key defence response to pathogen attack in plants is the induction and accumulation of various PR proteins, which also contribute to systematically acquired resistance [36, 37]. The PR-1, PR-2 [38], PR-3, PR-4, PR-5 [39], PR-9 [40], PR-10 [41], PR-11 [42], and PR-17 [43] families are associated with acquired resistance to pathogen infections. Among the genes encoding these PR proteins, *PR-1* is generally considered a marker gene for disease resistance [44]. In this study, PR-related genes were both significantly up- and downregulated in the mutant plants (Table 3), implying that *cis*-abienol may participate in TbCSV resistance in tobacco plants. Future research could assess disease resistance in *NtCPS2*-knockout and -overexpressing mutants to clarify the contribution of *cis*-abienol to tobacco disease resistance.

Conclusions

In this study, a genome-wide transcription profile was obtained for *NtCPS2*-knockout tobacco plants edited using CRISPR-Cas9. *NtCPS2* is a key gene for *cis*-abienol biosynthesis in tobacco. Genes involved in the biosynthesis of *cis*-abienol, early metabolites of GA, and carotenoids (including ABA) were significantly differentially expressed after *NtCPS2* knockout. The expression of PR-related genes also changed in response to low *cis*-abienol contents. Our findings may be useful for further investigations of

the molecular mechanisms associated with *NtCPS2* gene function and those underlying the regulation of related genes. Additionally, our results can contribute to the development of high-aroma tobacco varieties.

Methods

Tobacco Plant Culture

The tobacco plant variety (*N. tabacum* cv. 8306) used in this study produces high-aroma, flue-cured tobacco with high levels of *cis*-abienol. Plants were grown on a farm with loamy tidal soil near Henan Agricultural University, Zhengzhou City, China (136°56'6"E, 35°9'5"N) (113.63E, 37.75N). Transgenic tobacco plants were cultured and grown in mixed soil (1:1 vermiculite:humus) in a growth chamber at 22 °C with 250–300 μmol/m^2/s of photosynthetically available radiation and a 16-h light/8-h dark cycle. Measurements of leaf age started when the length of the middle leaf of each plant reached 1.5 cm. At a leaf age of 60 days, five tobacco plants at the same developmental stage from each treatment group were selected, and the middle leaves were sampled for the measurements of morphological characteristics and RNA extraction. Seeds were collected at 25 days after flowering. The plant materials are available at Henan Agricultural University. The formal identification of the plant materials was undertaken by the corresponding and first authors of this article. No voucher specimen of this material has been deposited in a publicly available herbarium.

Vector Construction

Based on the mRNA sequences and corresponding genome sequences, two CRISPR target sites (Supplementary Table 1) were designed to improve gene-targeting efficiency. Target primers for PCR (Supplementary Table 2) were designed and synthesised. After primer synthesis, fragments containing the target sites were amplified using overlap-extension PCR. The amplified fragments were cloned into a CRISPR expression vector using a recombinant enzyme from Nanjing Novozan Biotechnology Co., Ltd. (Nanjing, China). The CRISPR vector was electroporated into *Escherichia coli*, and positive clones were screened using colony PCR for *Agrobacterium tumefaciens*-mediated transformation and tobacco gene transformation.

Agrobacterium-mediated Transformation

Agrobacterium tumefaciens-mediated transformation was performed as follows: 5 μL of recombinant plasmid was mixed with 50 μL of competent *Agrobacterium tumefaciens* cells on ice for 30 min. Blank YEB medium was added, and the mixture was incubated at 28 °C for 12–13 h. Then, the mixture was transferred to YEB solid medium containing 50 mg/L of kanamycin and incubated at 28 °C for 36–48 h. Mature tobacco seeds were sterilised by washing with 75% alcohol and 10% sodium hypochlorite and placed into a germination medium. The seeds were then grown under light for 45 days. Samples with a diameter of 0.5 cm were taken from leaves with a hole punch, transferred to a pre-culture medium, and incubated for 2 days under light. *Agrobacterium tumefaciens* was activated in the medium containing

50 mg/L of kanamycin. Leaf discs were infected with *Agrobacterium tumefaciens*, transferred to a co-culture medium, and left for 3 days. Thereafter, the leaf discs were washed with sterilised distilled water and antibiotics in an aqueous solution. After the leaves were dried, they were transferred to a screening medium and cultured under light. After differentiation, they were transferred to a rooting medium. Transformed plants were obtained via rooting culture and transplanted into soil after 1 month.

DNA Extraction and Sequencing for Detecting Mutations in the Target Gene

Leaflets were collected from each plant, and genomic DNA was extracted using a standard cetrimonium bromide protocol. NPTII specific primers were used to detect successfully transformed plants via PCR (Supplementary Table 3). After confirming that the exogenous DNA fragment had been inserted, the primer 17KN48 was designed based on the *NtCPS2* gene sequence and target-site location to detect positive plants using PCR. PCR amplification was performed in the following reaction volume: 1 μL DNA, 2 μL 10 × PCR buffer, 0.4 μL dNTP mixture, 0.2 μL forward and reverse primers, 0.2 μL rTaq DNA polymerase (TOYOBO, Osaka, Japan), and 20 μL of diethyl pyrocarbonate-treated water. PCR was carried out using the following program: 94 °C for 3 min, 94 °C for 30 s, 55 °C for 30 s, 72 °C for 30 s, 72 °C for 10 min, and 25 °C for 1 min for 30 cycles. The PCR products were detected using gel electrophoresis and sequenced.

Measurements of Morphological Characteristics of Transgenic Tobacco Plants

Homozygous T_2 tobacco plants were selected, and morphological parameters including plant height, number of leaves, stem girth, internode length, and length and width of the largest leaf were measured at a leaf age of 60 days. The morphology of leaf glandular trichomes was also characterised. The largest leaves of each plant with the same age were detached, and the epidermis at the centre of each leaf was peeled off to examine the glandular trichomes using an Axioplan 2 microscope (Carl Zeiss, Oberkochen, Germany). The numbers of long and short glandular trichomes were counted and their lengths and diameters were measured. Each seedling had an average of approximately 100 glandular trichomes.

Analysis of Diterpenoids in Leaf Exudates Using GC-MS

Leaf exudates were sampled from fresh tobacco leaves, and 1:1 portions of the samples were directly injected into a 6890 N gas chromatograph coupled to a 5973 N mass spectrometer (Agilent Technologies, Santa Clara, CA, USA) for GC-MS analysis. Tobacco diterpenoids were identified based on their mass spectra.

RNA-seq Analysis

Total RNA was extracted from frozen leaf samples using TRIzol reagent (Invitrogen, Carlsbad, CA, USA) according to the manufacturer's protocol. RNA integrity was assessed using agarose gel electrophoresis, and RNA purity was checked using a NanoPhotometer® spectrophotometer (Implen, Munich, Germany).

RNA concentration was quantified with a Qubit®2.0 Flurometer using a Qubit® RNA Assay kit (Life Technologies, Carlsbad, CA, USA). From each qualified sample, 3 μg of RNA was sent to Illumina (San Diego, CA, USA) for sequencing. The cDNA library was prepared for sequencing according to the Illumina TruSeqTM RNA Sample Kit protocol. Sequencing was performed using an Illumina HiSeq 2500 system. RNA-seq reads were generated and processed to calculate expression levels, which were averaged over three biological replicates.

Bioinformatics Analysis of RNA-seq Data

Raw reads were processed through in-house Perl scripts. Clean reads were obtained by removing adapter-containing reads, reads containing ploy-N, and low-quality reads from the raw reads. The clean reads were then mapped to the tobacco reference genome (ftp://anonymous@ftp.solgenomics.net/genomes/Nicotiana_tabacum/assembly/K326). Using Hisat2 v2.0.5 (ftp://ftp.ensembl.org/pub/release-94/gtf/mus_musculus/), an index of the reference genome was built, and paired-end clean reads were aligned to the reference genome. We selected Hisat2 as the mapping tool because it can generate a database of splice junctions based on the gene model annotation file and thus produce better mapping results than other non-splice mapping tools. The expression level of each gene was normalised to fragments per kilobase per million for comparison among different samples. Differential expression analysis was performed using the DESeq2 R package (1.16.1) [47], and an absolute $\log_2$(FC) value > 1 and a corrected *p*-value < 0.05 were set as the thresholds for DEGs for subsequent analysis.

DEGs were further annotated using GO functional enrichment analysis. GO terms with corrected *p*-values < 0.05 were considered to be significantly enriched for a given DEG. Clusters of orthologous groups and pathway analyses were performed using KEGG (http://www.genome.jp/kegg) analytical tools. We used the clusterProfiler R package [48] to test the statistical enrichment of KEGG pathways for the DEGs. Data was showed in Supplementary Table 5.

Validation of DEGs Using qRT-PCR

The differential expression of 30 genes between wild-type and transgenic tobacco leaf samples was confirmed using qRT-PCR analysis with three biological replicates per sample. Primer sets for the DEGs were designed using Primer Premier 5.0 (Premier Biosoft, San Francisco, CA, USA) and synthesised by Invitrogen Trading (Shanghai) Co., Ltd. (China). All primer sequences are listed in Supplementary Table 4. RNA isolation, cDNA synthesis, qRT-PCR, and statistical analyses were performed as previously described [45]. Expression levels of the DEGs were normalised to that of the internal control gene L25 [46].

Statistical Analyses

Data are presented as the means ± standard deviations. Two-sample t-tests were used to compare the means between two treatments. Comparisons across multiple treatments were performed using one-way analysis of variance followed by Tukey’s honestly significant difference post-hoc test with SPSS v19

software (IBM Corporation, Armonk, NY, USA). A value of $p < 0.05$ was taken to denote statistical significance.

Abbreviations

CPS: Copalyl diphosphate synthase

DEG: Differentially expressed gene

ABS: cis-abienol synthase

KSL: kaurene synthase-like

KS: ent-Kaurene synthase

KO: ent-Kaurene oxidase

PSY: Phytoene synthases

LCY: Lycopene epsilon cyclases

KEGG: Kyoto Encyclopedia of Genes and Genomes

GO: Gene Ontology

8-OH-CPP: 8-Hydroxy-copalyl diphosphate

CDPK: Calcium-dependent protein kinase

GGPP: Geranyl diphosphate

PPPP: Prephytoene diphosphate

Declarations

Ethics approval and consent to participate

Not applicable.

Consent for publication:

Not applicable.

Availability of data and materials

Competing interests:

The authors declare no conflict of interest.

Funding

This research was funded by the Open Project Program of Key Laboratory of Tobacco Biology &Processing, Ministry of Agriculture, Qingdao, grant number (266101), China National Tobacco Corporation (110201402004; 110201002008), China National Tobacco Corporation Henan company (2018410000270035) and Guizhou Tobacco Corporation Guiyang company (2016-07). The funder had no role in study design, data collection and analysis, decision to publish, or preparation of the manuscript.

Author's Contributions

Conceptualization, S.X., G.X. and T.Y.; methodology, C.C. and L.H.; software, D.C. and L.H.; validation, T.Y.; formal analysis, J.S. and S.X.; investigation, D.C., L.H. and T.Y.; data curation, J.S. and S.X.; writing—original draft preparation, G.X.; writing—review and editing, Q.X., S.X. and T.Y.; funding acquisition, T.Y. All authors have read and agreed to the published version of the manuscript.

Acknowledgments:

We thank Yongle Ding and Zhaoyun Wu for their help.

References

1. Popova V, Ivanova T, Prokopov T, Nikolova M, Stoyanova A, Zheljazkov VD. Carotenoid-related volatile compounds of tobacco (*Nicotiana tabacum* L.) essential oils. Molecules 2019; 24(19).
2. Wagner GJ. Elucidation of the functions of genes central to diterpene metabolism in tobacco trichomes using posttranscriptional gene silencing. Planta. 2003;216(4):686–91.
3. Yan N, Du Y, Liu X, Zhang HB, Liu YH, Zhang P, Gong DP, Zhang ZF. Chemical structures, biosynthesis, bioactivities, biocatalysis and semisynthesis of tobacco cembranoids: An overview. Ind Crops Prod. 2016;83:66–80.
4. Koyama H, Kaku Y, Ohno M. Synthesis of ambrox from L-abietic acid. Tetrahedron Lett. 1987;28:2863–6.
5. Barrero AF, Alvarez-Manzaneda EJ, Altarejos J, Salido S, Ramos JM. Synthesis of ambrox(R) from (-)-sclareol and (+)-cis-abienol. Tetrahedron. 1993;49:10405–12.
6. Bolster MG, Jansen BJM, Groot A. The synthesis of (-)-Ambrox((R)) starting from labdanolic acid. Tetrahedron. 2001;57:5657–62.
7. Lin Y, Wagner GJ. Surface disposition and stability of pest-interactive, Trichome-exuded diterpenes and sucrose esters of Tobacco. J Chem Ecol. 1994;20:1907–21.
8. Kennedy BS, Nielsen MT, Severson RF. Biorationals from nicotiana protect cucumbers against colletotrichum-lagenarium (Pass) Ell and halst-disease development. J Chem Ecol. 1995;21:221–31.

9. Kennedy BS, Nielsen MT, Severson RF, Sisson VA, Stephenson MK, Jackson DM. Leaf surface chemicals from Nicotiana affecting germination of Peronospora-Tabacina (Adam) Sporangia. J Chem Ecol. 1992;18:1467–79.
10. Tomita H, Sato M, Kawashima N. Inheritance of labdanoid producing ability in *Nicotiana tabacum*. Agric Biol Chem. 1980;44:2517–8.
11. Wagner G. Leaf surface chemistry. In Tobacco Production, Chemistry and Technology. Blackwell Science 1999; 292–303.
12. Kubo T, Sato M, Tomita H, Kawashima N. Identification of the chromosome carrying the gene for cis-abienol production by the use of monosomics in *Nicotiana tabacum* L. Tob Int. 1982;184(23):57–9.
13. Vontimitta V, Danehower DA, Steede T, Moon HS, Lewis RS. Analysis of a Nicotiana tabacum L.genomic region controlling two leaf surface chemistry traits. J Agr Food Che. 2010;58(1):294–300.
14. Falara V, Pichersky E, Kanellis AK. A Copal-8-ol Diphosphate synthase from the angiosperm cistus creticus subsp creticus is a putative key enzyme for the formation of pharmacologically active, oxygen-containing labdane-type diterpenes. Plant Physiol. 2010;154(1):301–10.
15. Zerbe P, Chiang A, Yuen M, Hamberger B, Hamberger B, Draper JA, Britton R, Bohlmann J. Bifunctional cis-abienol synthase from Abies balsamea discovered by transcriptome sequencing and its implications for diterpenoid fragrance production. J Biol Chem. 2012;287:12121–31.
16. Sallaud C, Giacalone C, Töpfer R, Goepfert S, Bakaher N, Rösti S, Tissier A. Characterization of two genes for the biosynthesis of the labdane diterpene *Z*-abienol in tobacco (*Nicotiana tabacum*) glandular trichomes. Plant J. 2012;72:1–17.
17. Carman RM, Duffield AR. The biosynthesis of labdanoids – the optical purity of naturally-occuring manool and abienol. Aust J Chem. 1993;46:1105–14.
18. Guo ZH, Wagner GJ. Biosynthesis of labdenediol and sclareol in cell-free extracts from trichomes of *Nicotiana glutinosa*. Planta. 1995;197(4):627–32.
19. Cui H, Zhang ST, Yang HJ, Ji H, Wang XJ. Gene expression profile analysis of tobacco leaf trichomes. BMC Plant Biol. 2011;11(1):76.
20. Wang EM, Gan SS, Wagner GJ. Isolation and characterization of the CYP71D16 trichome-specific promoter from *Nicotiana tabacum* L. J Exp Bot. 2002;53(376):1891–7.
21. Severson RF, Arrendale RF, Chortyk OT, Johnson AW, Gwynn GR, Chaplin JF, Stephenson MG. Quantitation of the major cuticular components from green leaf of different Tobacco types. J Agr Food Che. 1984;32(3):1023–30.
22. Jinek M, Chylinski K, Fonfara I, Hauer M, Doudna JA, Charpentier E. A programmable dual-RNA-guided DNA endonuclease in adaptive bacterial immunity. Science. 2012;337:816–21.
23. Li JF, Norville JE, Aach J, McCormack M, Zhang D, Bush J, Church GM, Sheen J. Multiplex and homologous recombination-mediated genome editing in *Arabidopsis* and *Nicotiana benthamiana* using guide RNA and Cas9. Nat. Biotechnol. 2013;31:688–91.

24. Peng D, Tarleton R. EuPaGDT: a web tool tailored to design CRISPR guide RNAs for eukaryotic pathogens. Microbial genomics 2015; 1(4).
25. Helliwell CA, Sullivan JA, Mould RM, Gray JC, Peacock WJ, Dennis ES. A plastid envelope location of Arabidopsis ent -kaurene oxidase links the plastid and endoplasmic reticulum steps of the gibberellin biosynthesis pathway. Plant J. 2001;28:201–8.
26. Hedden P, Phillips AL. Gibberellin metabolism: new insights revealed by the genes. Trends Plant Sci. 2000;5:523–30.
27. Seo S, Gomi K, Kaku H, Ab H, Seto H, Nakatsu S, Neya M, Kobayashi M, Nakaho K, Lchinose Y. Identification of natural diterpenes that inhibit bacterial wilt disease in tobacco, tomato and arabidopsis. Plant Cell Physiol. 2012;53(8):1432–44.
28. Poovaih BW, Reddy ASN. Calcium and signal transduction in plants. Crit Rev Plant Sci. 1993;12:185–211.
29. Takahashi N, Phinney BO, MacMillan J, editors. Gibberellins. New York: Springer-Verlag; 1991.
30. Yamaguchi S. Gibberellin metabolism and its regulation. Annu Rev Plant Biol. 2008;59:225–51.
31. Yamaguchi S, Sun TP, Kawaide H, Kamiya Y. The GA2 locus of *Arabidopsis thaliana* encodes ent-kaurene synthase of gibberellin biosynthesis. Plant Physiol. 1998;116:1271–8.
32. Fleet CM, Yamaguchi S, Hanada A, Kawaide H, David CJ, Kamiya Y, Sun TP. Overexpression of *AtCPS* and *AtKS* in *Arabidopsis* confers increased ent-kaurene production but no increase in bioactive gibberellins. Plant Physiol. 2003;132:830–9.
33. Hedden P, Phillips AL, Rojas MC, Carrera E, Tudzynski B. Gibberellin biosynthesis in plants and fungi: a case of convergent evolution? J. Plant Growth Regul. 2002;20:319–31.
34. Kennedy BS, Nielsen MT, Severson RF, Sisson VA, Stephenson MK, Jackson DM. Leaf surface chemicals from Nicotiana affecting germination of Peronospora - Tabacina (Adam) Sporangia. J Chem Ecol. 1992;18(9):1467–79.
35. Severson R, Johnson A, Jackson D. Cuticular constituents of tobacco: factors affecting their production and their role in insect and disease resistance and smoke quality. Recent Adv Tobacco Sci. 1985;11:105–74.
36. Van LL, Rep M, Pieterse CM. Significance of inducible defense-related proteins in infected plants. Annu Rev Phytopathol. 2006;44:135–62.
37. Li K, Wu G, Li M, Ma M, Du J, Sun M, Qing L. Transcriptome analysis of *Nicotiana benthamiana* infected by Tobacco curly shoot virus. Virology J. 2018;15(1):138.
38. Bhat S, Folimonova SY, Cole AB, Ballard KD, Lei Z, Watson BS, Sumner LW, Nelson RS. Influence of host chloroplast proteins on Tobacco mosaic virus accumulation and intercellular movement. Plant Physiol. 2013;161:134–47.
39. Mochizuki T, Ogata Y, Hirata Y, Ohki ST. Quantitative transcriptional changes associated with chlorosis severity in mosaic leaves of tobacco plants infected with Cucumber mosaic virus. Mol Plant Pathol. 2014;15:242–54.

40. Xu Y, Zhou XP. Role of rice stripe virus NSvc4 in cell-to-cell movement and symptom development in Nicotiana benthamiana. Front Plant Sci. 2012;3:269.
41. Kong LF, Wu JX, Lu LN, Xu Y, Zhou XP. Interaction between Rice stripe virus disease-specific protein and host PsbP enhances virus symptoms. Mol Plant. 2014;7:691–708.
42. Balasubramaniam M, Kim BS, Hutchens-Williams HM, Loesch-Fries LS. The photosystem II oxygen-evolving complex protein PsbP interacts with the coat protein of Alfalfa mosaic virus and inhibits virus replication. Mol Plant Microbe Interact. 2014;27:1107–18.
43. Bhattacharyya D, Chakraborty S. Chloroplast: the Trojan horse in plant-virus interaction. Mol Plant Pathol. 2017;19:504–18.
44. Ryals JA, Neuenschwander UH, Willits MG, Molina A, Steiner HY, Hunt MD. Systemic acquired resistance. Plant Cell. 1996;8:1809–19.
45. Lu J, Du ZX, Kong J, Chen LN, Qiu YH, Li GF, Zhu SF. Transcriptome analysis of Nicotiana tabacum infected by cucumber mosaic virus during systemic symptom development. PLoS One. 2012;7:e43447.
46. Schmidt GW, Delaneym SK. Stable internal reference genes for normalization of real-time RT-PCR in tobacco (*Nicotiana tabacum*) during development and abiotic stress. Mol Genet Genom. 2010;283:233–41.
47. Varet H, Brilletguéguen L, Coppée JY, Dillies MA. SARTools: a DESeq2- and EdgeR-based R pipeline for comprehensive differential analysis of RNA-Seq data. PLoS One. 2016;11:e0157022.
48. Yu G, Wang LG, Han Y, He QY. ClusterProfiler: an R package for comparing biological themes among gene clusters. Omi AJ Integr Biol. 2011;16:284–7.

Figures

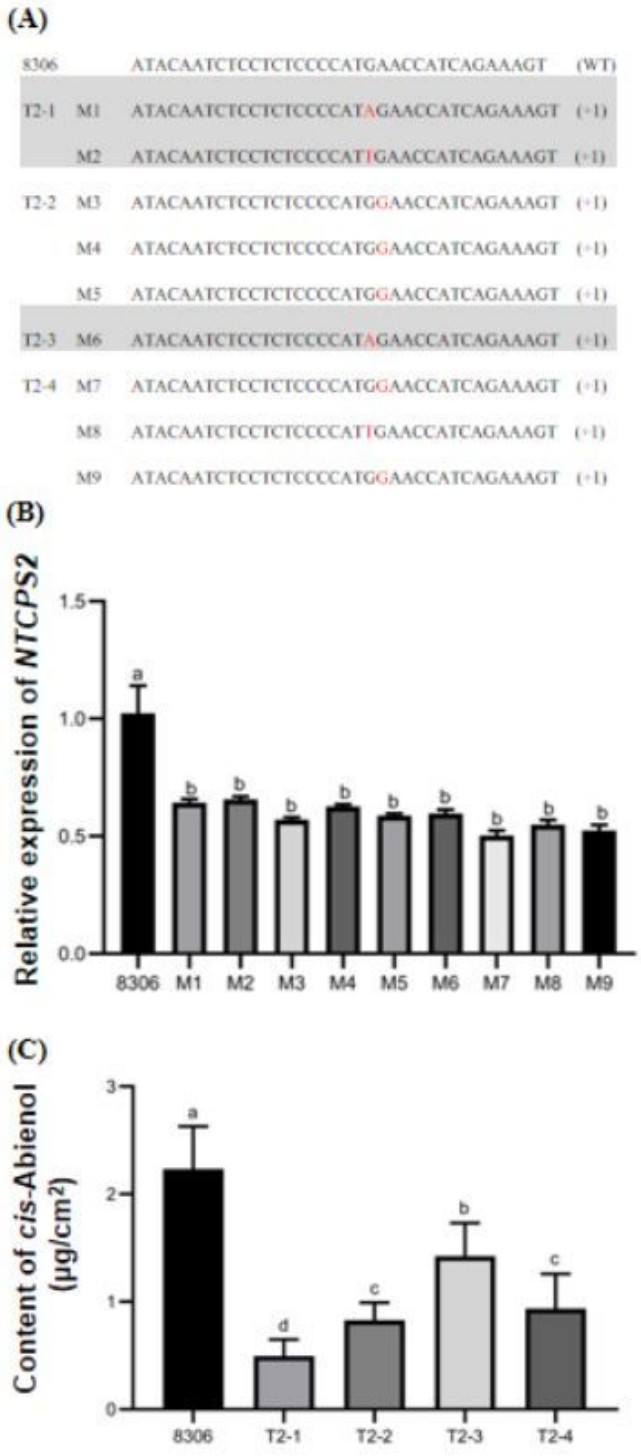

Figure 1

CRISPR/Cas9-induced mutations in T2 transgenic tobacco plants. (A) Sequences reflecting targeted inversions in the mutants. (B) Relative expression of NTCPS2 in the mutants. (C) Quantification of cis-abienol in homozygous T2 transgenic tobacco plants. Values are averages of at least three different plants or three different leaves.

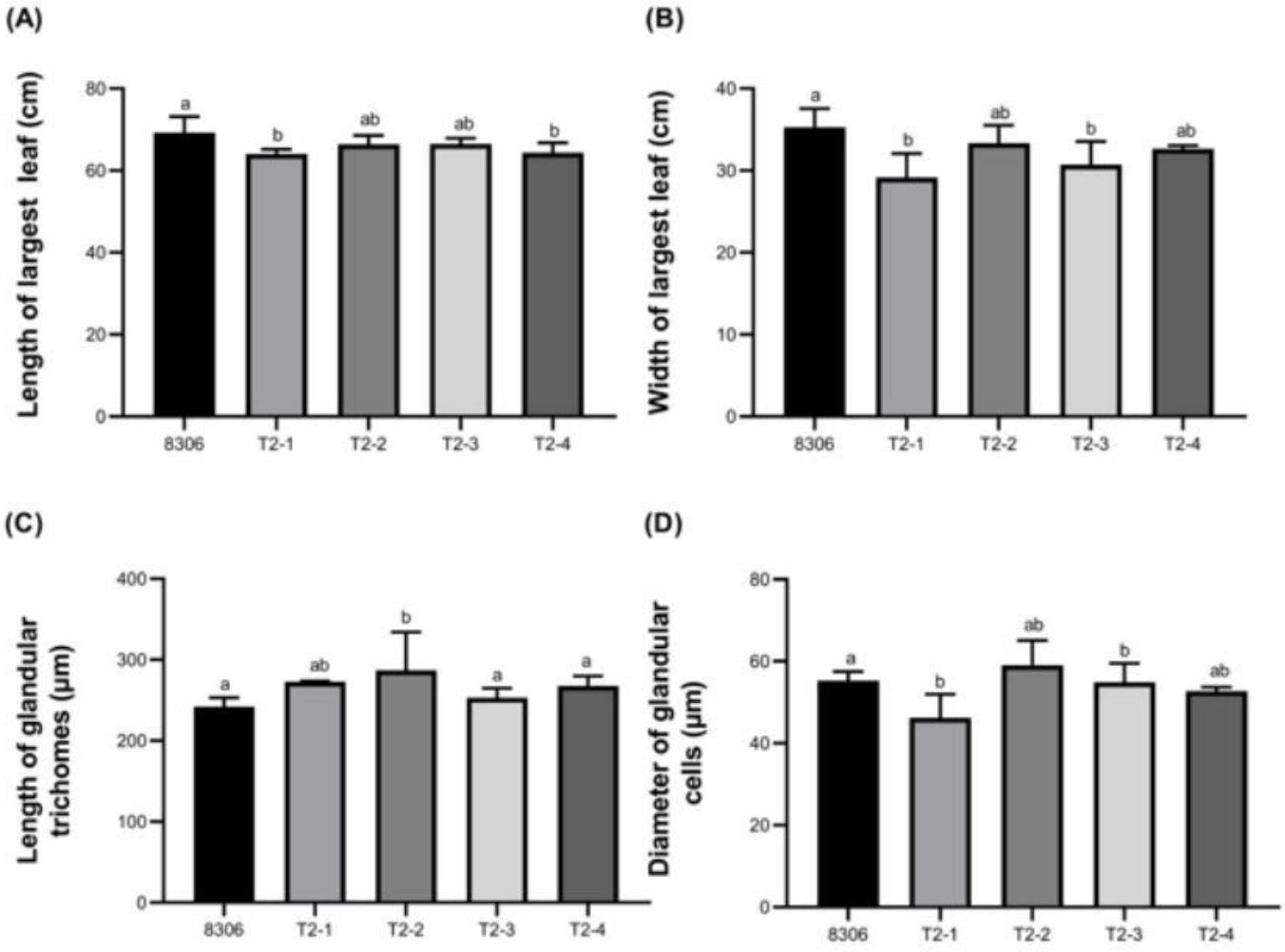

Figure 2

Morphological characteristics of mutant and wild-type plants, including the length (A) and width (B) of the largest leaf, length of glandular trichomes (C), and diameter of glandular cells (D). Values are presented as the means ± standard deviations (n = 4 for leaves and n = 100 for glandular trichomes). Different lowercase letters denote significant differences among plant lines ($p < 0.05$).

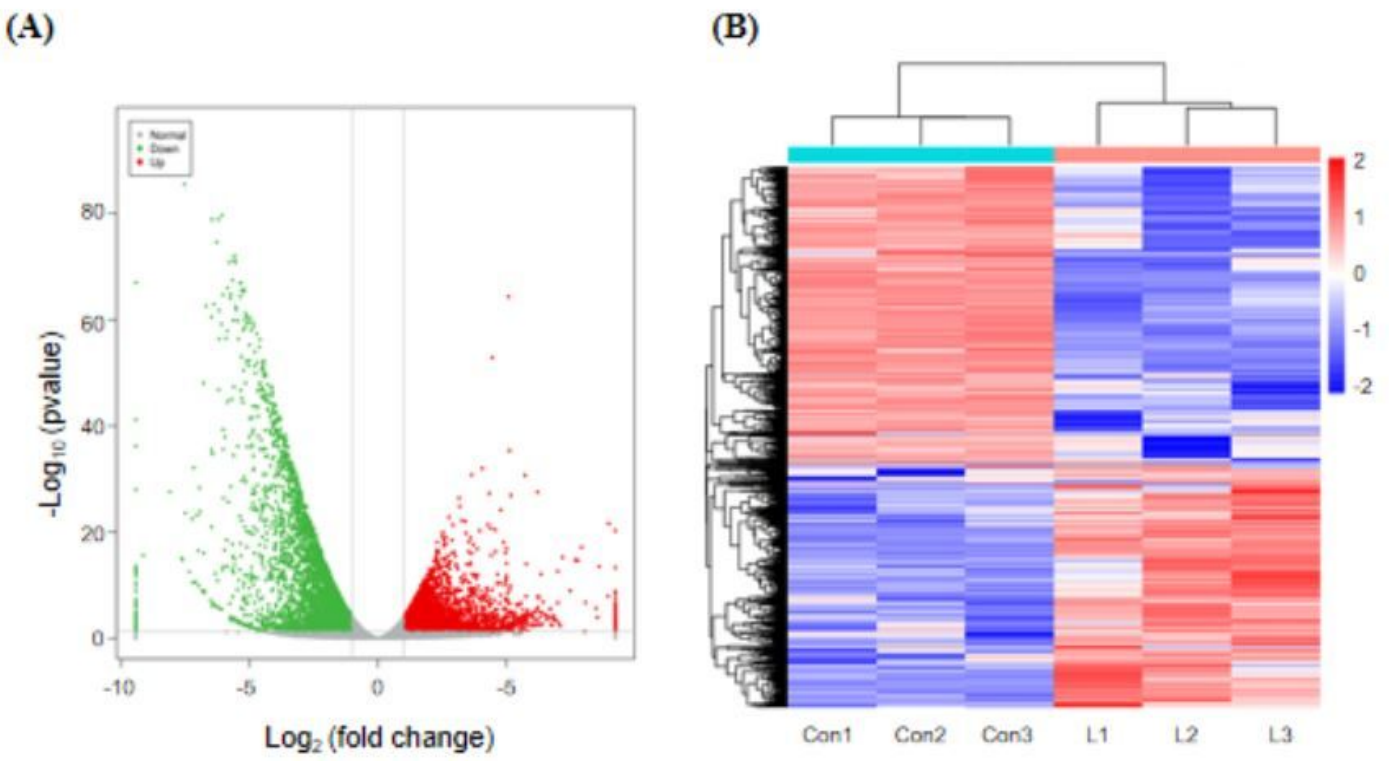

Figure 3

Differentially expressed genes (DEGs) were screened using the criteria fold change ≥ 2.0 and false discovery rate < 0.05. Significant differences in expression were observed for 9,514 genes, as represented by a volcano plot (A) and heat map (B).

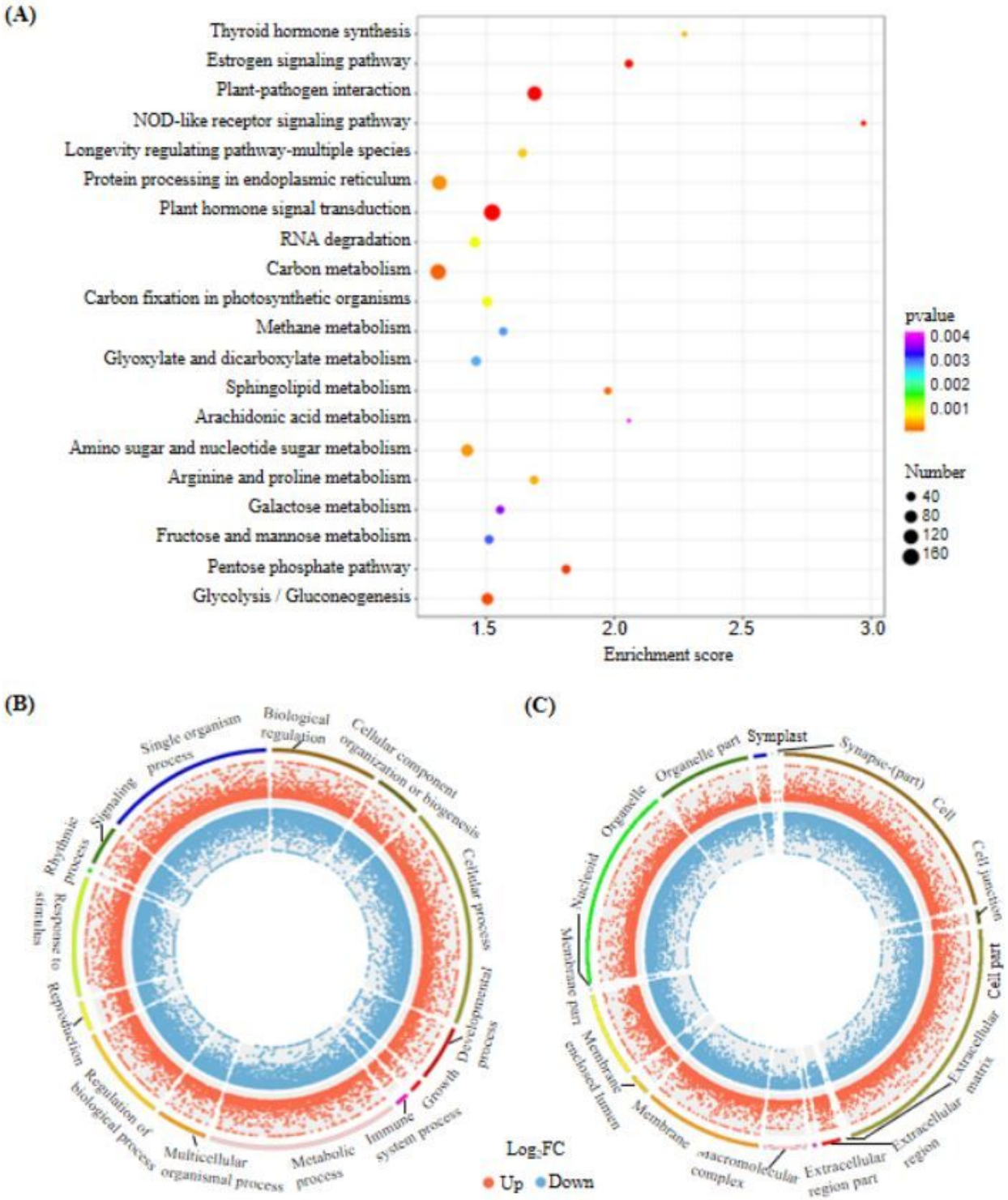

Figure 4

Kyoto Encyclopedia Gene and Genomes (KEGG) and Gene Ontology (GO) pathway analyses of DEGs after NtCPS2 knockout. (A) The top 20 enrichment scores for KEGG pathway enrichment analysis of differentially expressed mRNAs. (B) GO annotations of DEGs assigned to the biological processes category. (C) GO annotations of DEGs assigned to the cellular components category.

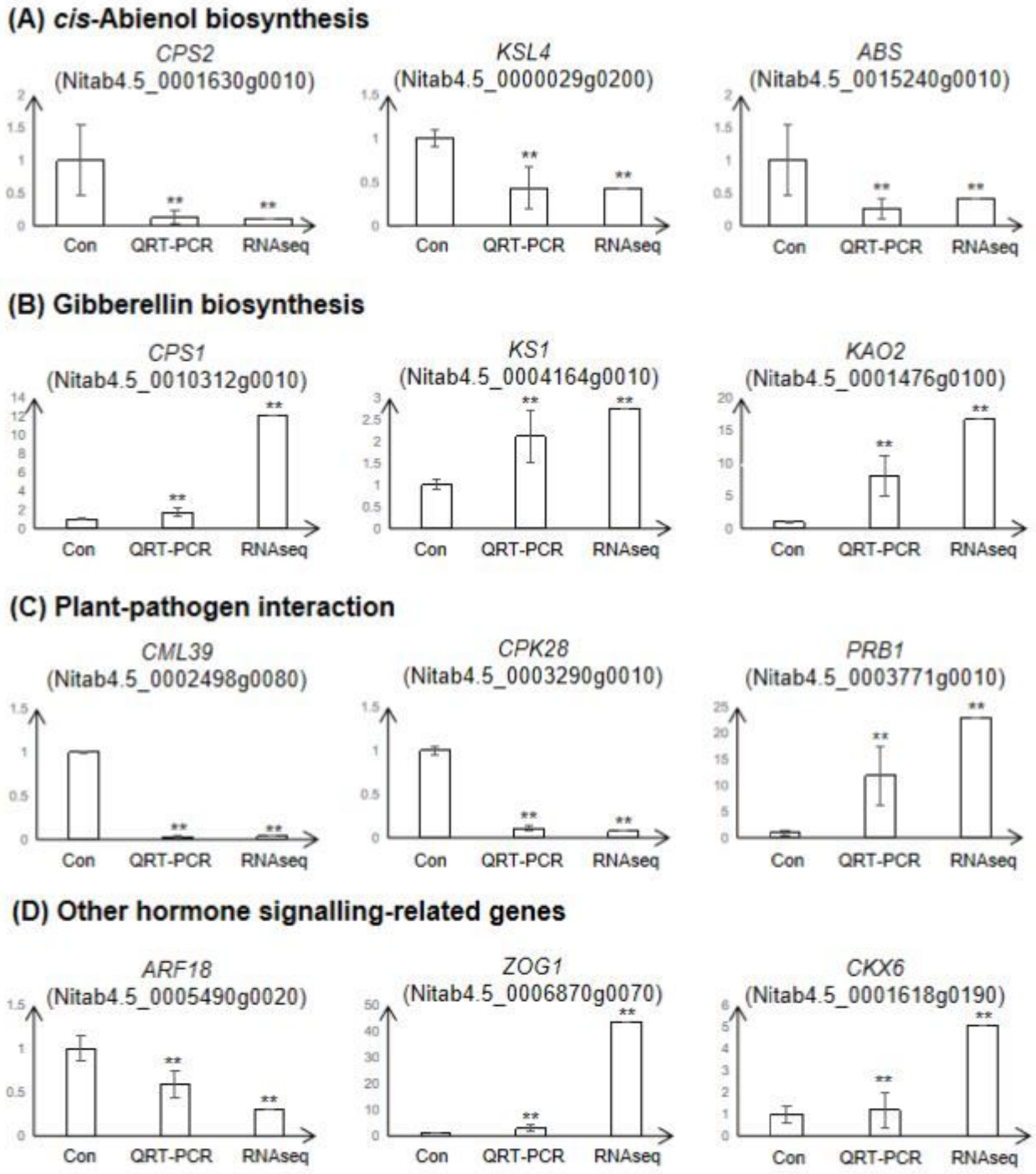

Figure 5

Transcription profiles of selected genes in mutant and wild-type plants as determined using RNA-seq and quantitative real-time polymerase chain reaction (QRT-PCR). Relative transcription levels of DEGs involved in cis-abienol biosynthesis (A), gibberellin (GA) biosynthesis (B), plant-pathogen interactions (C), and other hormone-signalling pathways (D). Asterisks indicate significant differences between samples and the control ($p < 0.05$, two-sample t-test).

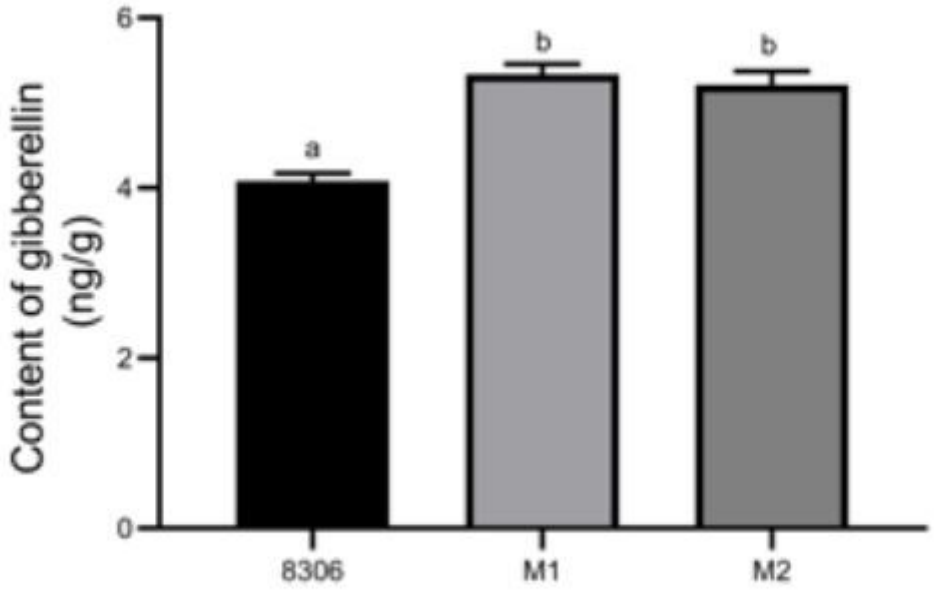

Figure 6

Gibberellin contents in the leaves of NtCPS2-knockout (M1 and M2) and wild-type (8306) tobacco. Different lowercase letters denote significant differences among plant strains ($p < 0.05$).

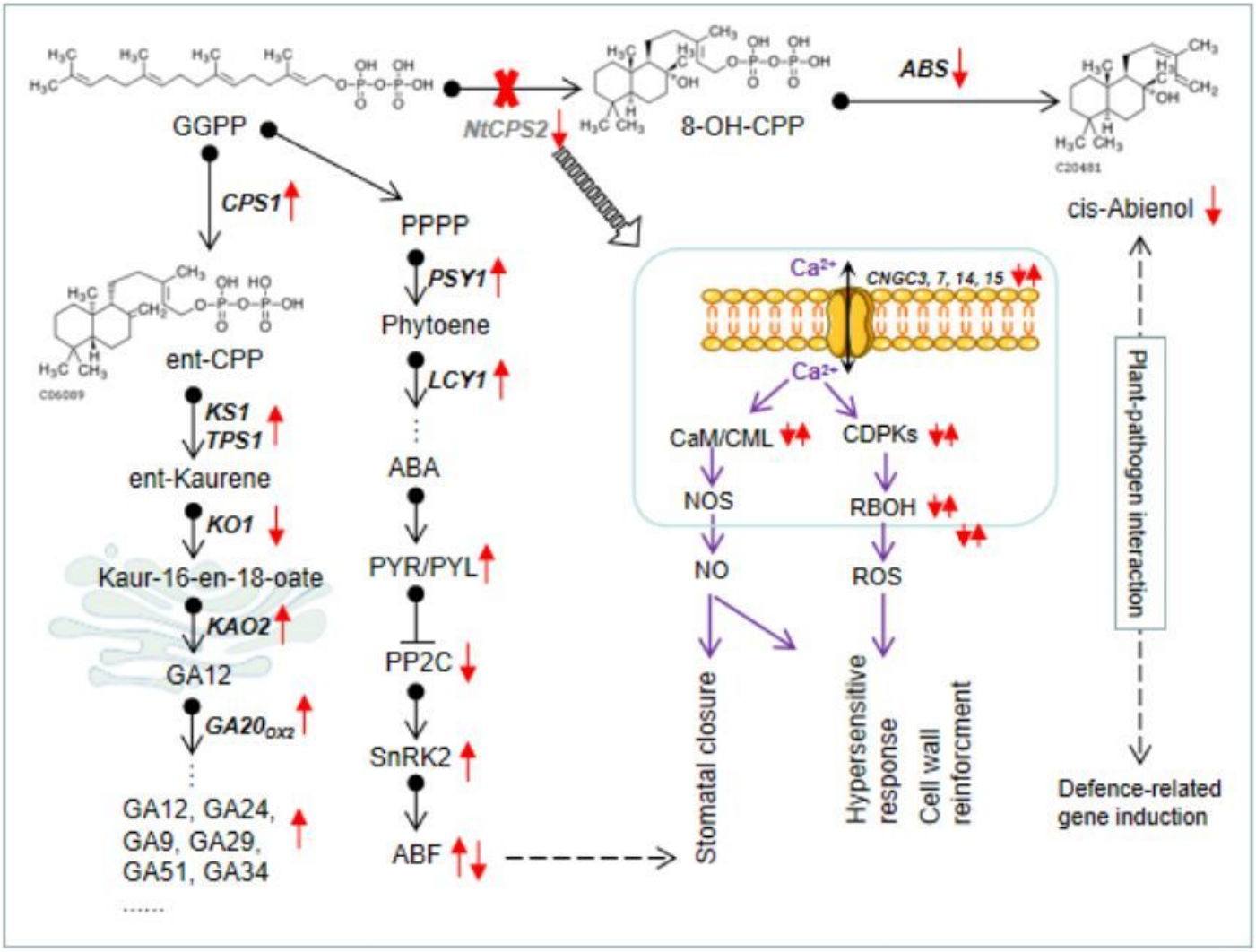

Figure 7

The changes in metabolic pathways associated with NtCPS2 knockout in tobacco. 8-OH-CPP, 8-hydroxy-copalyl diphosphate; ABA, abscisic acid; ABS, cis-abienol synthase; CDPK, calcium-dependent protein kinase; CPS1, copalyl diphosphate synthase 1; GGPP, geranyl diphosphate; LCY1, lycopene epsilon cyclase 1; NO, nitric oxide; NOS, nitric oxide synthase; PP2C, protein phosphatase 2C; PPPP, prephytoene diphosphate; PSY1, phytoene synthase 1; RBOH, rubidium hydroxide; ROS, reactive oxygen species; SnRK2, serine/threonine-protein kinase 2.

Supplementary Files

This is a list of supplementary files associated with this preprint. Click to download.

- Additionalfile1.docx
- SupplementaryFigure2.tif

- SupplementaryFigure1.tif
- SupplementaryTable5.xlsx
- SupplementaryTable4.xls
- SupplementaryTable3.xls
- SupplementaryTable2.xls
- SupplementaryTable1.xls